

Analytical and grid-free solutions to the Lighthill-Whitham-Richards traffic flow model

Pierre-Emmanuel Mazaré^a, Christian G. Claudel^b, Alexandre M. Bayen^c

^aCorresponding author. University of California at Berkeley, Transportation Engineering, Department of Civil and Environmental Engineering. Sutardja Hall 642, UC Berkeley, Berkeley, CA 94720-1710

^bUniversity of California at Berkeley, Department of Electrical Engineering and Computer Sciences. Sutardja Hall 621, UC Berkeley, Berkeley, CA 94720-1710.

^cUniversity of California at Berkeley, Systems Engineering, Department of Civil and Environmental Engineering. Sutardja Hall 642, UC Berkeley, Berkeley, CA 94720-1710

Abstract

In this article, we propose a computational method for solving the Lighthill-Whitham-Richards (LWR) partial differential equation (PDE) semi-analytically for arbitrary piecewise-constant initial and boundary conditions, and for arbitrary fundamental diagrams. For piecewise-constant initial and boundary conditions, and arbitrary fundamental diagrams, we show that the solution to the LWR PDE at any location and time can be computed exactly and semi-analytically for a very low computational cost using the cumulative number of vehicles formulation of the problem. We implement the proposed computational method on a representative traffic flow scenario to illustrate the exactness of the analytical solution. The computational cost of the method is shown to be lower than the cost of the Godunov scheme (also known as Cell Transmission Model in the transportation engineering literature). A toolbox implementation available for public download is briefly described, and posted at <http://traffic.berkeley.edu/downloads/>.

Key words: LWR model, traffic flow, grid-free numerical scheme, variational method

1. Introduction

1.1. Background

One of seminal traffic flow models for highways is presented in [27] and [33], and results in the so called *Lighthill-Whitham-Richards* (LWR) model or *kinematic wave* theory. Although more sophisticated models of traffic flow are available, the LWR model is widely used to model highway traffic [32] and more recently for urban traffic [18]. The LWR *partial differential equation* (PDE) is a first order scalar hyperbolic conservation law that computes the evolution of a density function (the density of vehicles on a road section). This PDE has multiple solutions in general, among which the entropy solution [2] is recognized to be the physically meaningful solution.

The LWR PDE can be numerically solved using a variety of computational methods, such as first order numerical schemes, for instance in [19, 10, 11]. Classical numerical methods often require a computational grid, and yield an approximate solution of the PDE. Some exceptions exist however, such as the wave tracking methods, see for instance [21, 28]. In the present article, we propose a new algorithm for solving the LWR PDE that does not require a computational grid, and which can be used to compute exactly the solutions to the LWR PDE for any concave fundamental diagram, and for any piecewise constant initial and boundary conditions semi-analytically.

Email addresses: mazare@berkeley.edu (Pierre-Emmanuel Mazaré), claudel@eecs.berkeley.edu (Christian G. Claudel), bayen@ce.berkeley.edu (Alexandre M. Bayen)

The algorithm presented in this article uses the *cumulative number of vehicles* [32] function (CVN function) as an intermediate computational abstraction. The CVN function is the integral form of the density function, and solves a Hamilton-Jacobi (HJ) PDE [13, 14], while the density function itself solves the LWR PDE. As the solution to a Hamilton-Jacobi equation with concave Hamiltonian, the CVN function can be computed at any point by minimizing a functional (or cost function), see [12, 4] for more details. An approximate minimization can be done numerically for example using *dynamic programming* (DP), which is used in [13]. The present article is also based on the variational method as [13], but unlike the latter, does not use a dynamic programming approximation for solving the HJ PDE.

We assume that the data used to simulate traffic evolutions is generated by *Eulerian* (fixed) sensors. This measurement data yields initial and boundary conditions, which are here assumed to be piecewise constant. *Lagrangian* data (originating from mobile sensors) could also be used as *internal boundary conditions* [25], but this is outside the scope of this article. Instead of solving the LWR PDE directly, we compute the solution to the corresponding HJ PDE, as well as its derivatives using a semi analytic method.

To the best knowledge of the authors, only front tracking [28, 21] and dynamic programming [13] methods can compute the solutions to the LWR PDE exactly, for specific classes of initial/boundary conditions and fundamental diagrams. The proposed method extends these computational methods for situations in which the initial/boundary conditions are piecewise constant and the fundamental diagram is an arbitrary concave function. Unlike the front-tracking methods, our computational method is not event-based, and can compute the solution at any given point without any knowledge or computation of prior events. Unlike dynamic programming methods used to compute the CVN function, our computational method is exact and can also compute the derivatives of the CVN function (that is, the solution to the LWR PDE) exactly, whereas the former method require (inexact) numerical differentiation. Most notably, the proposed method does not require to grid the space-time domain to compute the solution at a given point provided by the user.

Note that this method could also be extended to more complex initial/boundary conditions (for instance piecewise linear [28]), at the expense of a greater complexity. Symmetrically, we show in this article that the method can be simplified in the case of triangular fundamental diagrams. Triangular fundamental diagrams are of great importance and relevance for modeling and control applications, see [13, 10] for instance.

The rest of this article is organized as follows. Section 2 defines the LWR and HJ PDEs investigated in this article. Section 3 introduces the concept of partial solutions, which are used later as building blocks of the solution to the HJ PDE. In this section, we also show that the partial solutions can be computed analytically for any concave fundamental diagram (smooth or not). We also compute the solution to the LWR PDE on a traffic flow scenario to illustrate the algorithm's exactness, and compare its computational cost with the Godunov scheme (a first-order finite difference scheme). The properties of the resulting solution are investigated in Section 4. Finally, Section 5 presents a fast algorithm specific to triangular fundamental diagrams, for which additional simplifications can be made.

2. Modeling

2.1. The LWR PDE

We quickly summarize standard material related to the LWR PDE and its connection to the Hamilton-Jacobi PDE through the so-called Moskowitz equation. We consider a one-dimensional, uniform section of highway, limited by x_0 upstream and x_n downstream. For a given time $t \in [0, t_m]$ and position $x \in [x_0, x_n]$, we define the local traffic density $k(x, t)$ in vehicles per unit length, and the instantaneous flow $q(x, t)$ in vehicles per unit time. The conservation of vehicles on the highway is written as follows [27, 33, 17]:

$$\forall x, t \in [x_0, x_n] \times [0, t_m], \quad \frac{\partial k(x, t)}{\partial t} + \frac{\partial q(x, t)}{\partial x} = 0 \quad (1)$$

For first order traffic flow models, flow and density are related by the *fundamental diagram* $Q : (x, t, k(x, t)) \mapsto q(x, t)$, which is an empirically measured law [20]. Through this article, we consider the homogeneous problem [14] in which the fundamental diagram is a function of density k only, i.e. $q(x, t, k(x, t)) = Q(k(x, t))$.

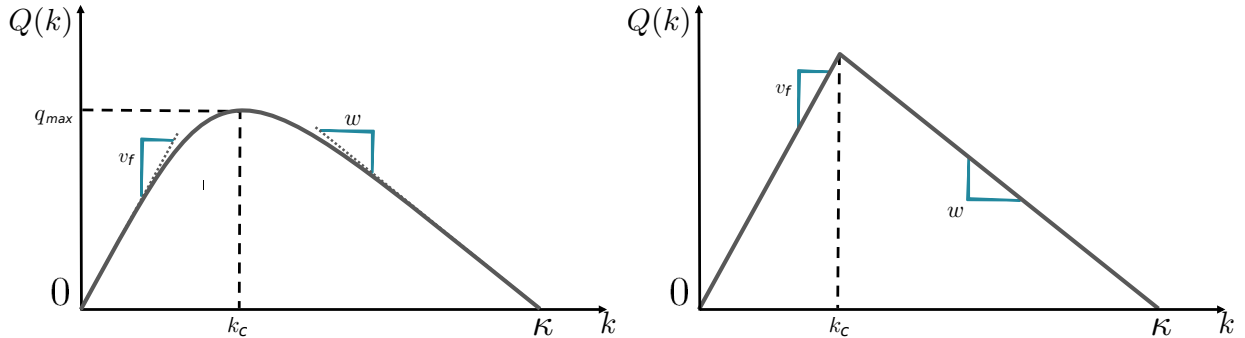


Figure 1: **Left:** Generic concave fundamental diagram. **Right:** Triangular fundamental diagram.

The fundamental diagram is a positive function defined on $[0, \kappa]$, where κ is the maximal density (jam density). It ranges in $[0, q_{\max}]$ where q_{\max} is the maximum flow (capacity). It is assumed to be differentiable at 0 and κ , with $Q'(0) = v_f > 0$ the free flow speed, and $Q'(\kappa) = w < 0$ the congested wave speed [27]. We assume that the fundamental diagram is concave and continuous. Both assumptions are not dictated by physical laws but are required for the mathematical well-posedness of the approach. Non-concave and non-continuous fundamental diagrams are sometimes necessary to model specific traffic patterns [24, 15] but they require a separate mathematical treatment. Examples of fundamental diagrams satisfying all the above assumptions are shown in Fig. 1.

The introduction of the fundamental diagram yields the *Lighthill-Whitham-Richards (LWR) PDE*:

$$\forall x, t \in [x_0, x_n] \times [0, t_m], \quad \frac{\partial k(x, t)}{\partial t} + \frac{\partial Q(k(x, t))}{\partial x} = 0 \quad (2)$$

2.2. The Moskowitz function

The cumulated vehicle count $\mathbf{N}(x, t)$, also called Moskowitz function [30], represents the continuous vehicle count at location x and time t . It has been developed for instance in [32, 13, 14] in the context of transportation engineering, and goes back to [29, 30].

In the Moskowitz framework, one assumes that all vehicles are labeled by increasing integers as they pass the entry point x_0 of a highway section, and that they cannot pass each other. If the latest car that passed an observer standing at location x and time t is labeled n , then $\lfloor \mathbf{N}(x, t) \rfloor = n$. This count function is interpolated continuously between the discrete labels. The Moskowitz function contains traffic information that one can infer from experimental traffic measurements as long as vehicles do not pass each other. In this situation, the isolines of $\mathbf{N}(x, t)$ correspond to vehicle trajectories.

Moreover, local density $k(x, t)$ and flow $q(x, t)$ can be computed from the vehicle count using the equalities

$$k(x, t) = -\frac{\partial \mathbf{N}(x, t)}{\partial x} \quad (3)$$

$$q(x, t) = \frac{\partial \mathbf{N}(x, t)}{\partial t} \quad (4)$$

Introducing the Moskowitz function in (2) yields the *Hamilton-Jacobi PDE* [32, 13, 14, 8, 9] in which the fundamental diagram Q plays the role of Hamiltonian [16]:

$$\frac{\partial \mathbf{N}(x, t)}{\partial t} - Q\left(-\frac{\partial \mathbf{N}(x, t)}{\partial x}\right) = 0 \quad (5)$$

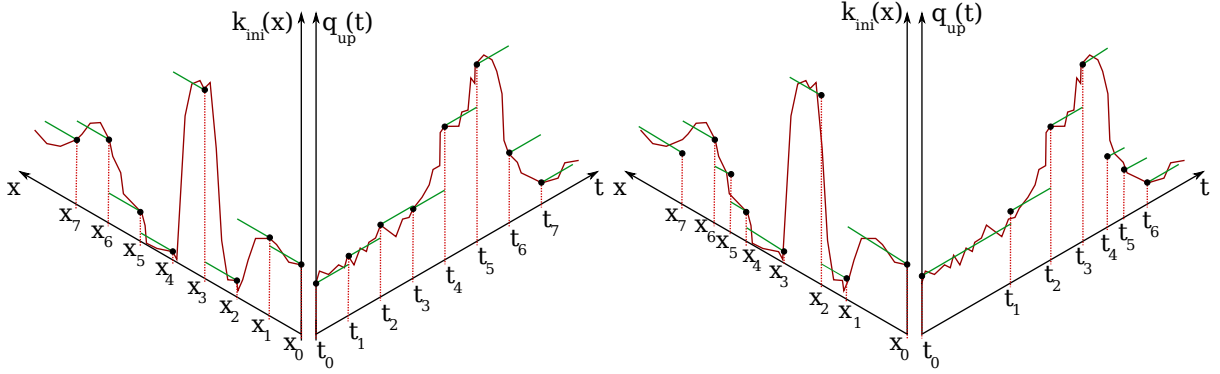


Figure 2: Different piecewise-constant encodings of the same noisy initial condition k_{ini} and upstream boundary condition q_{up} . For clarity, the downstream boundary condition has not been included in this figure. **Left:** example of uniformly sampled k_{ini} and q_{up} , leading to $x_i = i\delta x$ and $t_j = j\delta t$. **Right:** example of unevenly spaced x_i and t_i .

2.3. The Cauchy problem

Equation (5) is a scalar Hamilton-Jacobi partial differential equation, which can be solved using an initial condition function $\mathbf{N}_{\text{ini}}(x)$, an upstream boundary condition function $\mathbf{N}_{\text{up}}(t)$ and a downstream boundary condition function $\mathbf{N}_{\text{down}}(t)$. In general, finding such solutions while enforcing arbitrary boundary conditions is impossible with experimental data because the data is not necessarily consistent with the model, and contains measurement errors, leading to ill-posed problems. Weak boundary conditions were introduced in [5, 26, 34] to resolve this problem by integrating situations in which prescribed boundary conditions do not apply. In the context of the Hamilton-Jacobi equation, we can introduce the Cauchy problem:

$$\forall x, t \in [x_0, x_n] \times [0, t_m], \quad \begin{cases} \frac{\partial \mathbf{N}(x, t)}{\partial t} - Q \left(-\frac{\partial \mathbf{N}(x, t)}{\partial x} \right) = 0 \\ \mathbf{N}(x, 0) \doteq \mathbf{N}_{\text{ini}}(x) \\ \mathbf{N}(x_0, t) \doteq \mathbf{N}_{\text{up}}(t) \\ \mathbf{N}(x_n, t) \doteq \mathbf{N}_{\text{down}}(t) \end{cases} \quad (6)$$

where \doteq represents the imposition of a weak boundary condition as developed in [34]. Note that weak boundary conditions are related to the concept of demand and supply, see for instance [10, 11].

2.4. Piecewise affine initial and boundary conditions

For the rest of the article, we use piecewise constant conditions on density and flow, which translate to piecewise-affine conditions on the Moskowitz function. Piecewise constant conditions on density and flow are a natural way to encode discrete measurements in the model, and are used in the *Cell Transmission Model* (CTM) [10]. A graphical representation of the studied domain is shown in Fig. 2.

Let m and $n \geq 1$ be integers, $x_0 < x_1 < \dots < x_n$ and $t_0 < t_1 < \dots < t_m$ the space-time discretization for initial and boundary conditions where $t_0 = 0$. We assume that the initial densities $(k_{\text{ini}}^{(i)})_{0 \leq i \leq n-1} \in \mathbb{R}_+^n$, the upstream flows $(q_{\text{up}}^{(j)})_{0 \leq j \leq m-1} \in \mathbb{R}_+^m$ and the downstream flows $(q_{\text{down}}^{(j)})_{0 \leq j \leq m-1} \in \mathbb{R}_+^m$ are given (known), as in Figure 2. The initial densities are thus decomposed as piecewise constant in their respective measurement intervals:

$$\forall x \in [x_i, x_{i+1}[, \quad k(x, 0) = k_{\text{ini}}^{(i)} \quad (7)$$

and let the upstream and downstream flows also be prescribed as piecewise constant:

$$\forall t \in [t_j, t_{j+1}[, \quad q(x_0, t) = q_{\text{up}}^{(j)} \quad (8)$$

$$q(x_n, t) = q_{\text{down}}^{(j)} \quad (9)$$

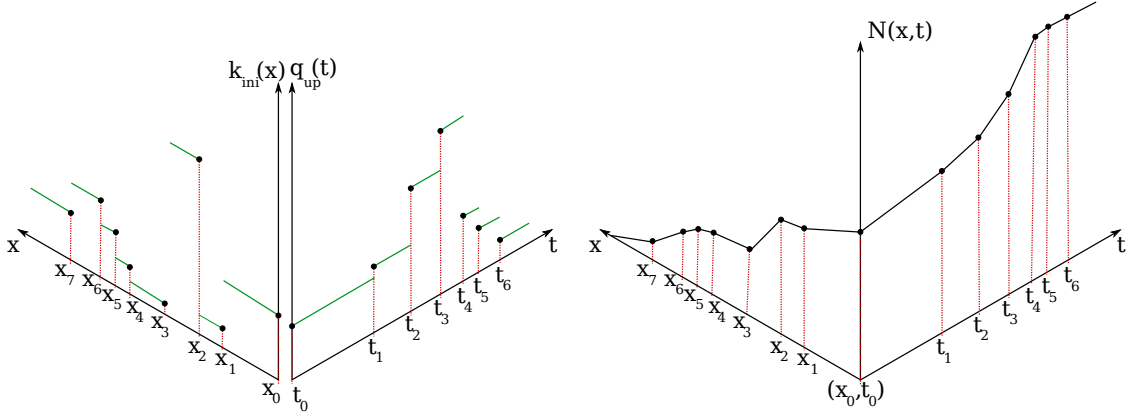


Figure 3: **Left:** illustration of a piecewise constant initial density and upstream flow conditions. **Right:** corresponding piecewise affine Moskowitz function. For clarity, downstream boundary conditions are not shown.

Note that no assumption is made regarding the uniformity of the grid: the spacings $x_i - x_{i-1}$ and $t_i - t_{i-1}$ are not necessarily uniform over i . The method proposed next can handle arbitrary grids and spatio-temporal discretization of the data. However, for notational simplicity, we will not write the method in its full generality in this article. In the toolbox posted online [37], we have coded a general implementation of the method which takes arbitrary measurement intervals $[x_i, x_{i+1}]$ and $[t_j, t_{j+1}]$.

The initial condition of the Moskowitz PDE is obtained by integrating the initial condition of the LWR PDE assuming that $\mathbf{N}_{\text{ini}}(x_0) = 0$ and :

$$\forall x \in [x_i, x_{i+1}], \mathbf{N}_{\text{ini}}(x) = - \int_{x_0}^x k(\chi, 0) d\chi = - \sum_{m=0}^{i-1} (x_{m+1} - x_m) k_{\text{ini}}^{(m)} - (x - x_i) k_{\text{ini}}^{(i)} \quad (10)$$

Similarly, the upstream and downstream boundary conditions of the Moskowitz PDE, assuming that $\mathbf{N}_{\text{up}}(0) = 0$ and $\mathbf{N}_{\text{ini}}(x_n) = \mathbf{N}_{\text{down}}(0)$ are given by:

$$\forall t \in [t_j, t_{j+1}], \mathbf{N}_{\text{up}}(t) = \int_0^t q_{\text{up}}(\tau) d\tau = \sum_{m=0}^{j-1} (t_{m+1} - t_m) q_{\text{up}}^{(m)} + (t - t_j) q_{\text{up}}^{(j)} \quad (11)$$

$$\forall t \in [t_j, t_{j+1}], \mathbf{N}_{\text{down}}(t) = \mathbf{N}_{\text{ini}}(x_n) + \int_0^t q_{\text{down}}(\tau) d\tau = \mathbf{N}_{\text{ini}}(x_n) + \sum_{m=0}^{j-1} (t_{m+1} - t_m) q_{\text{down}}^{(m)} + (t - t_j) q_{\text{down}}^{(j)} \quad (12)$$

3. Analytical solutions to the Moskowitz HJ PDE and LWR PDE

3.1. Solutions to the Hamilton-Jacobi equation

In order to compute the analytical solution of equation (6) with conditions of the type (10), (11), (12), we define (based on [8, 4]) the following convex transform associated with the fundamental diagram, also used by Daganzo [14]:

$$\forall u \in [w, v_f], \quad R(u) = \sup_{k \in [0, \kappa]} (Q(k) - u \cdot k) \quad (13)$$

Note that R is a convex function, since it is the supremum of affine functions. The function $-R$ is the Legendre-Fenchel transform of the function Q (fundamental diagram).

We aggregate the initial and boundary conditions into a single *value condition function* $\mathbf{c}(x, t)$:

$$\mathbf{c}(x, t) = \begin{cases} \mathbf{N}_{\text{ini}}(x) & t = 0 \\ \mathbf{N}_{\text{up}}(t) & x = x_0 \\ \mathbf{N}_{\text{down}}(t) & x = x_n \end{cases}$$

With this definition of initial, upstream and downstream boundary conditions, the domain of definition of \mathbf{c} is $\text{Dom}(\mathbf{c}) = (\{x_0, x_n\} \times [0, t_m]) \cup ([x_0, x_n] \times \{0\})$.

Variational theory as known since [1] is a possible method for solving the HJ PDE (5). A possible use of variational theory is presented in [12] in the context of this problem. The mathematical foundations of variational theory can be found in [4] for the specific case of the HJ PDEs. From [4], the solution associated with the value condition function \mathbf{c} , denoted by $N_{\mathbf{c}}$, is the infimum of an infinite number of functions of the value condition:

$$\begin{aligned} \mathbf{N}_{\mathbf{c}}(x, t) = & \inf \{ \mathbf{c}(t - T, x - Tu) + TR(u) \} \\ \text{s. t. } & (u, T) \in [w, v_f] \times \mathbb{R}_+ \text{ and } (t - T, x - Tu) \in \text{Dom}(\mathbf{c}) \end{aligned} \quad (14)$$

Equation (14) is well known in the Hamilton-Jacobi literature and often referred to as Lax-Hopf formula [4, 16]. Note that it can be solved using dynamic programming methods [12], which are proven to be exact for homogeneous problems under two conditions: a concave, piecewise-affine fundamental diagram, and the computation of the Moskowitz function on a uniform grid $(j\delta x, i\delta t)_{i,j}$ which has to be invariant by any translation of vector $(\delta x, \delta x/w_i)$ for each wave speed w_i [12]. These conditions can be restrictive based on the data used for practical applications since they dictate a sampling frequency. Also, they can be computationally intensive.

In this article, we present a method which guarantees an analytical solution, and has the same computational complexity for arbitrary grids and concave fundamental diagrams. In addition, we show that this method enables us to compute the solution to the associated Cauchy problem (6) exactly.

For this, we first decompose the piecewise affine value condition function \mathbf{c} in affine, locally-defined value conditions indexed by *ini*, *up* and *down* based on the condition (initial, upstream, downstream), and *i* or *j* depending on the sampling interval:

$$\forall x \in [x_i, x_{i+1}[, \quad \mathbf{c}_{\text{ini}}^{(i)}(x, 0) = \mathbf{N}_{\text{ini}}(x) \quad (15)$$

$$\forall t \in [t_j, t_{j+1}[, \quad \mathbf{c}_{\text{up}}^{(j)}(x_0, t) = \mathbf{N}_{\text{up}}(t) \quad (16)$$

$$\forall t \in [t_j, t_{j+1}[, \quad \mathbf{c}_{\text{down}}^{(j)}(x_n, t) = \mathbf{N}_{\text{down}}(t) \quad (17)$$

where \mathbf{N}_{ini} , \mathbf{N}_{up} and \mathbf{N}_{down} are defined in (10),(11),(12). One can note that the functions $\mathbf{c}_{\text{ini}}^{(i)}$, $\mathbf{c}_{\text{up}}^{(j)}$ and $\mathbf{c}_{\text{down}}^{(j)}$ are restrictions of the piecewise-affine function \mathbf{c} on intervals on which it is affine. We also define the induced solution components $\mathbf{N}_{\mathbf{c}_{\text{ini}}^{(i)}}$, $\mathbf{N}_{\mathbf{c}_{\text{up}}^{(j)}}$ and $\mathbf{N}_{\mathbf{c}_{\text{down}}^{(j)}}$ respectively associated with (15),(16) and (17) when computed by (14) as follows. The induced solution components must be understood as the partial solution to a subset of the initial problem, since we assume that we have no information and do not impose any value on the other initial and boundary condition domains. The contribution of the present article is the construction of the full solution of the problem from these partial solutions.

In general, the Moskowitz function $\mathbf{N}_{\mathbf{c}}$, solving the HJ PDE (5) for the value condition \mathbf{c} , cannot be computed analytically using (14) for arbitrary piecewise affine initial and boundary conditions. However, the induced Moskowitz components defined above can be computed analytically using (14). These partial computations involve the minimization of a convex function [9] which we present later in the article. Using the minimum property [32], also known as inf-morphism property [4], the Moskowitz function $\mathbf{N}_{\mathbf{c}}$, solving the HJ PDE (5) for the value condition \mathbf{c} is the minimum of the induced Moskowitz components. This fundamental property [4] is the basis of the algorithm presented in this article.

3.2. Solution components associated with affine conditions

In this section, we use the notation Q' for the derivative of the fundamental diagram (which only depends on one argument). Note that we have assumed earlier that Q has a right derivative v_f in 0 and a left derivative

w in κ . A full mathematical treatment of these derivatives is available in [8, 9], using subgradients, which is outside of the scope of this article, but enables the proper treatment of nonsmooth fundamental diagrams such as the triangular diagram.

We now present the computation of the partial components of the solution.

3.2.1. Initial conditions

We want to compute the solution component induced by an affine, locally defined initial condition indexed by i :

$$\forall x \in [x_i, x_{i+1}], \quad \mathbf{N}_{\text{ini}}^{(i)}(x) = -k_i x + b_i \quad (18)$$

with $b_i = k_i x_i - \sum_{l=0}^{i-1} (x_{l+1} - x_l) k_{\text{ini}}^{(l)}$ allowing for the continuity of the initial conditions in $(0, x_i)$. Using the results of [9], the analytical solution to the problem associated with (6) with this sole initial condition can be written as

$$\mathbf{N}_{\text{c}_{\text{ini}}^{(i)}}(x, t) = \begin{cases} tQ(k_i) - k_i x + b_i & : x_i + tQ'(k_i) \leq x \leq x_{i+1} + tQ'(k_i) \\ tR\left(\frac{x-x_i}{t}\right) - k_i x_i + b_i & : x_i + tw \leq x \leq x_i + tQ'(k_i) \\ tR\left(\frac{x-x_{i+1}}{t}\right) - k_i x_{i+1} + b_i & : x_{i+1} + tQ'(k_i) \leq x \leq x_{i+1} + tv_f \end{cases} \quad (19)$$

$$k_{\text{c}_{\text{ini}}^{(i)}}(x, t) = -\frac{\partial \mathbf{N}_{\text{c}_{\text{ini}}^{(i)}}(x, t)}{\partial x} = \begin{cases} k_i & : x_i + tQ'(k_i) \leq x \leq x_{i+1} + tQ'(k_i) \\ -R'\left(\frac{x-x_i}{t}\right) & : x_i + tw \leq x \leq x_i + tQ'(k_i) \\ -R'\left(\frac{x-x_{i+1}}{t}\right) & : x_{i+1} + tQ'(k_i) \leq x \leq x_{i+1} + tv_f \end{cases} \quad (20)$$

3.2.2. Upstream boundary conditions

We now compute the solution component induced by an affine, locally defined upstream boundary condition indexed by j .

$$\forall t \in [t_j, t_{j+1}], \quad \mathbf{N}_{\text{up}}^{(j)}(t) = q_j t + d_j \quad (21)$$

with $d_j = k_j x_j + \sum_{l=0}^{j-1} (t_{l+1} - t_l) q_{\text{up}}^{(l)}$. Following [9], we define the freeflow density function K_{up} , which is the inverse of the restriction of the fundamental diagram Q to the domain $[0, k_c]$:

$$K_{\text{up}}(q) = \min\{k \in [0, \kappa] | Q(k) = q\}$$

Using the results of [9], one can prove that:

$$\mathbf{N}_{\text{c}_{\text{up}}^{(j)}}(x, t) = \begin{cases} d_j + q_j t_{j+1} + (t - t_{j+1})R\left(\frac{x-x_0}{t-t_{j+1}}\right) & : 0 \leq x - x_0 \leq Q'(K_{\text{up}}(q_j))(t - t_{j+1}) \\ d_j + q_j t - K_{\text{up}}(q_j)(x - x_0) & : Q'(K_{\text{up}}(q_j))(t - t_{j+1}) \leq x - x_0 \leq Q'(K_{\text{up}}(q_j))(t - t_j) \\ d_j + q_j t_j + (t - t_j)R\left(\frac{x-x_0}{t-t_j}\right) & : Q'(K_{\text{up}}(q_j))(t - t_j) \leq x - x_0 \leq v_f(t - t_j) \end{cases} \quad (22)$$

$$k_{\text{c}_{\text{up}}^{(j)}}(x, t) = -\frac{\partial \mathbf{N}_{\text{c}_{\text{up}}^{(j)}}(x, t)}{\partial x} = \begin{cases} -R'\left(\frac{x-x_0}{t-t_{j+1}}\right) & : 0 \leq x - x_0 \leq (t - t_{j+1})Q'(K_{\text{up}}(q_j)) \\ K_{\text{up}}(q_j) & : Q'(K_{\text{up}}(q_j))(t - t_{j+1}) \leq x - x_0 \leq Q'(K_{\text{up}}(q_j))(t - t_j) \\ -R'\left(\frac{x-x_0}{t-t_j}\right) & : Q'(K_{\text{up}}(q_j))(t - t_j) \leq x - x_0 \leq v_f(t - t_j) \end{cases} \quad (23)$$

3.2.3. Downstream boundary conditions

Finally, the same process can be repeated for the downstream boundary:

$$\forall t \in [t_j, t_{j+1}], \quad \mathbf{N}_{\text{down}}^{(j)}(t) = p_j t + b_j \quad (24)$$

with $b_j = k_j x_j + \sum_{l=0}^{j-1} (t_{l+1} - t_l) q_{\text{down}}^{(l)}$. In a symmetric way from the upstream case, we define the congestion density function K_{down} , which is the inverse of the restriction of the fundamental diagram Q to the domain $[k_c, \kappa]$:

$$K_{\text{down}}(q) = \max\{k \in [0, \kappa] | Q(k) = q\}$$

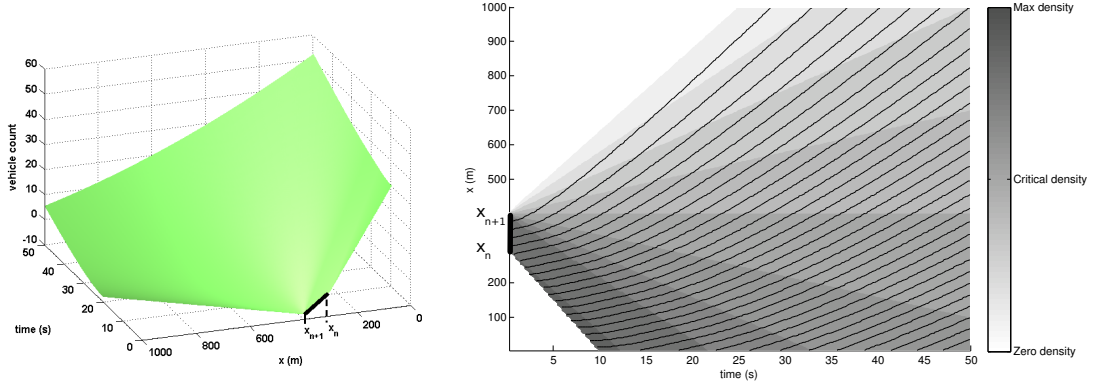


Figure 4: Example of affine initial condition (thick line in black) and induced solution component, for the Greenshields fundamental diagram. **Left:** Three-dimensional representation of the Moskowitz function. **Right:** Two-dimensional plot of the density and associated vehicle trajectories. Note that the visualization requires the calculation of the Moskowitz function on a regular grid for display purposes, but the algorithm does not: it can compute the value of the function at any arbitrary point (x, t) without computing it at nearby points or anywhere else. Solution obtained with toolbox [37].

Using the results of [9], we can similarly prove that:

$$\mathbf{N}_{\mathbf{c}_{\text{down}}^{(j)}}(x, t) = \begin{cases} b_j + p_j t + K_{\text{down}}(p_j)(x_n - x) & : Q'(K_{\text{down}}(p_j))(t - t_j) \leq x - x_n \leq Q'(K_{\text{down}}(p_j))(t - t_{j+1}) \\ b_j + p_j t_j + (t - t_j)R\left(\frac{x_n - x}{t_j - t}\right) & : w(t - t_j) \leq x - x_n \leq Q'(K_{\text{down}}(p_j))(t - t_j) \\ b_j + p_j t_{j+1} + (t - t_{j+1})R\left(\frac{x_n - x}{t_{j+1} - t}\right) & : Q'(K_{\text{down}}(p_j))(t - t_{j+1}) \leq x - x_n \leq 0 \end{cases} \quad (25)$$

$$k_{\mathbf{c}_{\text{down}}^{(i)}}(x, t) = -\frac{\partial \mathbf{N}_{\mathbf{c}_{\text{down}}^{(i)}}(x, t)}{\partial x} = \begin{cases} K_{\text{down}}(p_j) & : Q'(K_{\text{down}}(p_j))(t - t_j) \leq x - x_n \leq Q'(K_{\text{down}}(p_j))(t - t_{j+1}) \\ -R'\left(\frac{x_n - x}{t_j - t}\right) & : w \leq \frac{x_n - x}{t_j - t} \leq Q'(K_{\text{down}}(p_j)) \\ -R'\left(\frac{x_n - x}{t_{j+1} - t}\right) & : Q'(K_{\text{down}}(p_j))(t - t_{j+1}) \leq x - x_n \leq 0 \end{cases} \quad (26)$$

3.3. Componentwise computation of the Moskowitz/LWR function

It is shown in [3, 4] that one way to express the solution of the full problem (6), taking into account all contributions of initial and boundary conditions can be obtained by a union property of capture basins, called inf-morphism property. The inf-morphism property applied to the functions $(\mathbf{c}_{\text{ini}}^{(i)})_i$, $(\mathbf{c}_{\text{up}}^{(j)})_j$ and $(\mathbf{c}_{\text{down}}^{(j)})_j$, is expressed by the following equality:

$$\mathbf{N}(x, t) = \min_{i,j} \left\{ \mathbf{N}_{\mathbf{c}_{\text{ini}}^{(i)}}(x, t), \mathbf{N}_{\mathbf{c}_{\text{up}}^{(j)}}(x, t), \mathbf{N}_{\mathbf{c}_{\text{down}}^{(j)}}(x, t) \right\} \quad (27)$$

This last result is fundamental: it shows that in order to solve the HJ PDE, we only have to apply the formulas above (19,22,25) for each affine piece of initial and boundary condition, which will give the associated solution component, and then compute the minimum of all results.

3.4. Implementation

In the algorithm labeled Alg. 1, we summarize the proposed method for the computation of the Moskowitz function. The algorithm supposes the knowledge of the value conditions $k_{\text{ini}}^{(i)}$, $q_{\text{up}}^{(j)}$, $q_{\text{down}}^{(j)}$ and their boundaries x_i , t_j . Note that in order to preserve the exactness of the algorithm (i.e. the analytical expression of the solution), the explicit derivative of the fundamental diagram is necessary, which is easy for most commonly used fundamental diagrams.

We implemented this algorithm in Matlab code and used it to compute the solution of an arbitrary problem, and posted a manual with examples, so that the code can be directly accessible to users. The performance of the algorithm is illustrated for an arbitrary set of numerical values, summarized in the tables

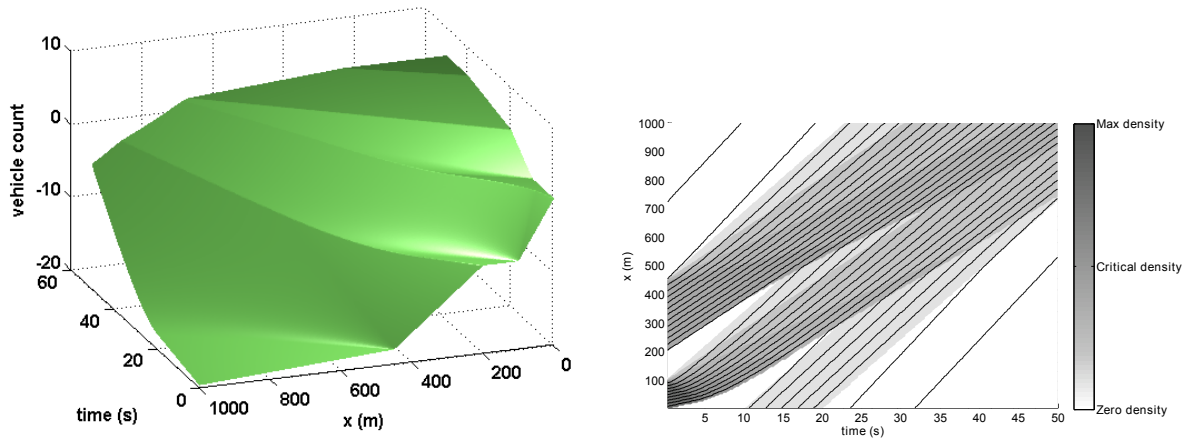


Figure 5: Exact solution to an arbitrary set of initial and value conditions, using a Greenshields fundamental diagram. **Left:** three-dimensional representation of the count function. **Right:** two-dimensional plot of the density and associated trajectories. Solution obtained with toolbox [37]

below. The NaN for the downstream boundary encodes the fact that no measurement was available at that point, which is a signature feature of the algorithm: it computes the solution to the problem with the prescribed data (and can circumvent missing data problems).

i	t_{i-1}	t_i	$q_{\text{up}}^{(i)}$	$q_{\text{down}}^{(i)}$
1	0	10	0	NaN
2	10	20	.4	NaN
3	20	40	.1	NaN
4	40	50	0	NaN

i	x_{i-1}	x_i	$k_{\text{ini}}^{(i)}$
1	0	100	.08
2	100	200	0
3	200	450	.04
4	450	1000	.003

The solution of the Cauchy problem associated with these value conditions and a Greenshields fundamental diagram [20, 17]: $Q(k) = kv_f(1 - k/\kappa)$, with $v_f = 30$ m/s the free-flow speed and $\kappa = .1$ veh/m the maximum capacity, is represented in Fig. 5.

As can be seen from the implementation of Alg 1 posted online [37], all what is required is to prescribe the data at $[x_0, x_1], \dots, [x_{n-1}, x_n]$ and $[t_0, t_1], \dots, [t_{m-1}, t_m]$ and the point (x, t) where one wants the solution.

4. Properties of the solution

4.1. Interpretation and analysis of the solution

4.1.1. Structure

Each solution component $\mathbf{N}_{\mathbf{c}^{(i)}}$ induced by a value condition $\mathbf{c}^{(i)}$ is defined in the convex domain:

$$\text{Dom}(\mathbf{N}_{\mathbf{c}^{(i)}}) = [x_0, x_n] \times [0, t_m] \cap \{(x + v\delta t, t + \delta t) | \delta t \geq 0, v \in [w, v_f], (x, t) \in \text{Dom}(\mathbf{c}^{(i)})\} \quad (28)$$

which is the union of all areas that are attainable by a characteristic starting from any point (x, t) of the value condition domain, and at an information propagation speed $v \in [w, v_f]$, sometimes also referred to as the reachable set. In equation (28), $\mathbf{c}^{(i)}$ can encode either an initial, upstream or downstream component.

A solution component induced by an affine value condition will generally consist of three different parts outlined in the bullet list below:

Algorithm 1 Pseudo-code implementation for the Lax-Hopf based computation of the Moskowitz function and the associated density at a single point (x, t) prescribed by the user.

Input: $x \in [x_0, x_n], t \in [0, t_m]$, {input space domain, time domain}

$i_{\text{up}} \leftarrow \min(i - 1)$ s.t. $t_i \geq t - \frac{x-x_0}{v_f}$ {number of components to compute from upstream data}
 $i_{\text{down}} \leftarrow \min(i - 1)$ s.t. $t_i \geq t - \frac{x_n-x}{w}$ {number of components to compute from downstream data}
 $j_{\text{min}} \leftarrow \max(0, \min(j - 1)$ s.t. $x_j \geq x - v_f t$) {min space index for influencing initial condition}
 $j_{\text{max}} \leftarrow \min(m, \max(j + 1)$ s.t. $x_j \leq x - wt$) {max space index for influencing initial condition}
 $\mathbf{N} \leftarrow +\infty$ {initialization of the Moskowitz function to infinity}

for $j = j_{\text{min}}$ **to** j_{max} **do** {iteration on initial conditions}

 compute $\mathbf{N}_{\mathbf{c}_{\text{ini}}^{(j)}}(x, t)$ using (19) {component induced by the initial condition $\mathbf{c}_{\text{ini}}^{(j)}$ }

if $\mathbf{N}_{\mathbf{c}_{\text{ini}}^{(j)}}(x, t) < \mathbf{N}$ **then** {if the current component contributes to the solution}

$\mathbf{N} \leftarrow \mathbf{N}_{\mathbf{c}_{\text{ini}}^{(j)}}(x, t)$ {update Moskowitz function}

$k \leftarrow k_{\mathbf{c}_{\text{ini}}^{(j)}}(x, t)$, computed using (20) {compute density}

end if

end for

for $i = 0$ **to** i_{up} **do** {iteration on upstream boundary conditions}

 compute $\mathbf{N}_{\mathbf{c}_{\text{up}}^{(i)}}(x, t)$ using (22) {component induced by the upstream boundary condition $\mathbf{c}_{\text{up}}^{(i)}$ }

if $\mathbf{N}_{\mathbf{c}_{\text{up}}^{(i)}}(x, t) < \mathbf{N}$ **then** {if the current component contributes to the solution}

$\mathbf{N} \leftarrow \mathbf{N}_{\mathbf{c}_{\text{up}}^{(i)}}(x, t)$ {update Moskowitz function}

$k \leftarrow k_{\mathbf{c}_{\text{up}}^{(i)}}(x, t)$, computed using (23) {compute density}

end if

end for

for $i = 0$ **to** i_{down} **do** {iteration on downstream boundary conditions}

 compute $\mathbf{N}_{\mathbf{c}_{\text{down}}^{(i)}}(x, t)$ using (25) {component induced by the downstream boundary condition $\mathbf{c}_{\text{down}}^{(i)}$ }

if $\mathbf{N}_{\mathbf{c}_{\text{down}}^{(i)}}(x, t) < \mathbf{N}$ **then** {if the current component contributes to the solution}

$\mathbf{N} \leftarrow \mathbf{N}_{\mathbf{c}_{\text{down}}^{(i)}}(x, t)$ {update Moskowitz function}

$k \leftarrow k_{\mathbf{c}_{\text{down}}^{(i)}}(x, t)$, computed using (26) {compute density}

end if

end for

Output: \mathbf{N}, k

- The *forward fan*: this characteristic fan starts at the most upstream point of the value condition. Shaped as a cone, it propagates at speeds $v \in [w, Q'(k)]$. It is a transition area where, on any given trajectory, the vehicle speed goes from zero to the vehicle speeds corresponding to the density imposed by the value condition, while the density decreases.
- The characteristic domain: this domain propagates at a speed $Q'(k)$, where k is either k_i , $K_{\text{up}}(q_i)$ or $K_{\text{down}}(q_i)$. In this area, vehicle speed and density are constant and match those imposed by the value condition.
- The *backward fan*: this wave starts at the most downstream point of the value condition. Shaped as a cone, it propagates at speeds $v \in [Q'(k), v_f]$. It is a transition area where, on a given trajectory, the vehicle speeds go from the value condition vehicle speeds to the free flow speed, while the density decreases.

This structure of the solution component induced by an affine initial condition is represented in Figure 6. The structure of the solution components induced by affine upstream (respectively downstream) affine boundary conditions is similar, with the exception of a missing backward (respectively forward) fan domain.

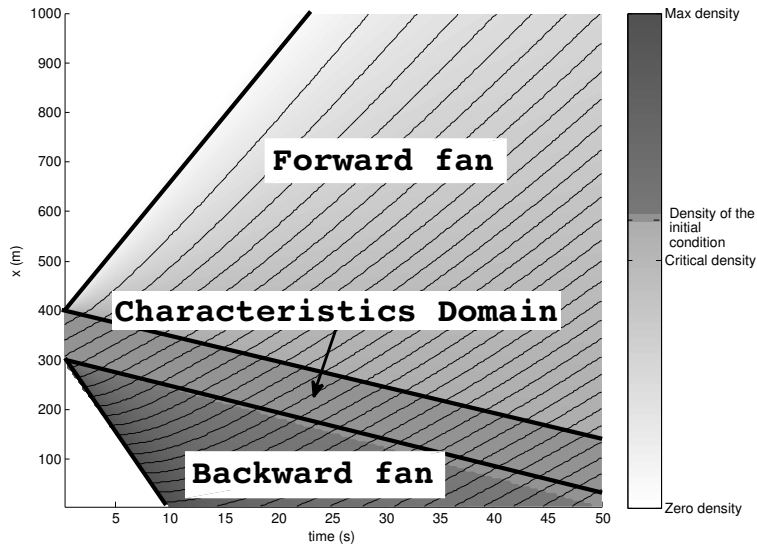


Figure 6: Density (gray levels) and vehicle trajectories (curves) from a solution component induced by a constant initial density between $x_i = 300m$ and $x_{i+1} = 400m$. The boundaries between the different portions of the solution component are represented by thick lines. Note that the characteristic domain exhibits a single density which is the density of the initial condition, and smooth compression and expansion are taking place respectively in the forward and backward characteristic fans. The area labeled as NaN is outside the domain of influence of the data between $x = 300m$ and $x = 400m$, thus, the component is not defined there. Solution computed using toolbox [37].

4.1.2. Flows and speeds associated with the solution components

Spatial derivatives are bounded, as shown by the analytical calculation of the densities in (20),(23),(26). From these equations, one can also obtain the flow and speed by using the classical formulas: $q(x, t) = Q(k(x, t))$ and

$$v(k) = \begin{cases} \frac{Q(k)}{k} & \text{if } 0 < k \leq \kappa \\ Q'(0) & \text{if } k = 0 \end{cases}$$

Note that the results of these inversions are only as good as the approximation used for the fundamental diagram. In particular, the fundamental diagram sometime fails to capture the variability of traffic in congestion [6, 35].

The convexity of the solution components has been proved in [9]. Each solution component is Lipschitz-continuous as long as the initial and boundary conditions are such that the imposed densities are positive and below the maximum density, and the imposed flows are positive and below the maximum flow. One can also note that as long as these conditions are met, the solution only exhibits positive flows. These conditions are equivalent to the *well-posedness* conditions introduced in [14].

4.2. Lipschitz-continuity of the solution

The Cauchy problem associated to the LWR PDE (6) is called a *well-posed problem* if the initial densities and upstream and downstream flows lie within their physically-imposed limits:

$$0 \leq k_{\text{ini}}^{(i)} \leq \kappa \quad (29)$$

$$0 \leq q_{\text{up}}^{(j)} \leq q_{\text{max}} \quad (30)$$

$$0 \leq q_{\text{down}}^{(j)} \leq q_{\text{max}} \quad (31)$$

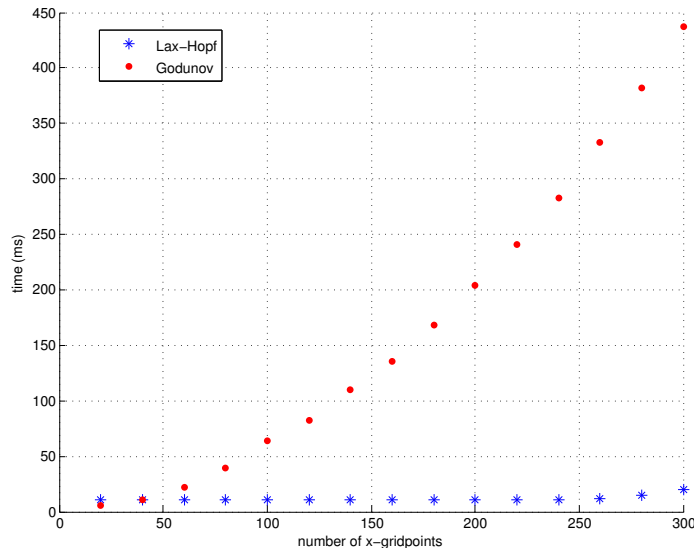


Figure 7: Computation times to compute the density field solution at time $t = 50s$ to an arbitrary Cauchy problem using two different methods: a Godunov scheme, and the proposed Lax-Hopf algorithm. The complexity of the numerical scheme increases quadratically with the desired granularity due to the CFL condition, whereas the computational cost of the Lax-Hopf algorithm sees a linear complexity, which appears constant at this scale.

The Lipschitz-continuity of the solution to such problems is proven in Appendix A. Interestingly, this proof relies solely on the form of the solution and not on the LWR PDE (though obviously the solution encodes the PDE in its structure). The interpretation is that despite the fact that the solution components are irregularly shaped, they are never strictly below the neighboring components on the edges of their domain of definition. This means that the solution has to be continuous, and the associated flow and density are respectively in $[0, q_{\max}]$ and $[0, \kappa]$.

As will be seen later, considering only well-posed problems allows for simplifications in the computation of the solution by reducing the number of solution components to consider during the computation.

4.3. Benefits of a grid-free method

This new method comes with several benefits: as a grid-free method, it does not require any intermediate computations (small steps) in order to give a forecast of the future traffic state. In general, for finite differences methods such as the CTM or the Godunov scheme, the constraint on the time-space grid spacing $\delta t, \delta x$ is defined by the CFL condition: $\frac{\delta x}{\delta t} \geq \sup_k |Q'(k)|$.

For instance, most traffic estimation applications require high resolution output such as $\delta x \leq 200m$, see for example [22, 36, 23, 31]. Input data, such as electromagnetic loops or probe data comes with a time granularity of $\delta t \geq 30s$. Working with a grid with $\delta t = 30s$ and $\delta x = 200m$ would be most efficient algorithmically, however the CFL constraint with $\sup_k |Q'(k)| = v_f = 33m/s$ imposes $\delta t \leq 6s$. Thus, to obtain a solution at a $200m$ resolution, $6s$ time steps are required. For finite differences schemes, this represents a five-fold increase in computational time. From an information point of view, this increase comes only from the finite-differences methods and reflects a mathematical limit of the approximation, which lies in the discretization method.

Our method, however, does not require a grid, and its complexity increases only linearly with the number of value conditions, i.e. the granularity of the boundary condition data. On the other hand, a finite differences method will see its complexity increase proportionally to the product of the maximum number of initial conditions and the maximum number of upstream or downstream conditions, since the minimum granularity of the value conditions is then the grid spacing.

5. Faster algorithm for triangular fundamental diagrams

5.1. Modeling

The triangular fundamental diagram Q is defined by:

$$Q(k) = \begin{cases} v_f k & : x \in [0, k_c] \\ w(k - \kappa) & : x \in [k_c, \kappa] \end{cases}$$

where

$$k_c = \frac{-w\kappa}{v_f - w}$$

is the density corresponding to the maximum capacity. This fundamental diagram is graphically represented in Fig. 1. The calculation of its convex transform R using (13) yields:

$$\forall u \in [w, v_f], R(u) = k_c(v_f - u)$$

Owing to the simplicity of the triangular fundamental diagram and its convex transform, the solution components associated with affine internal and boundary conditions can be calculated explicitly and lead to an even simpler set of results: for an initial condition $\mathbf{N}_{\text{ini}}^{(i)}$ as defined in (18), plugging the explicit convex transform into (19) yields two cases:

If $0 \leq k_i \leq k_c$, the initial condition imposes a free-flow state.

$$\mathbf{N}_{\text{c}_{\text{ini}}^{(i)}}(x, t) = \begin{cases} (i) & k_i(tv_f - x) + b_i & : x_i + tv_f \leq x \leq x_{i+1} + tv_f \\ (ii) & k_c(tv_f - x) + b_i + x_i(k_c - k_i) & : x_i + tw \leq x \leq x_i + tv_f \end{cases} \quad (32)$$

else, if $k_c < k_i \leq \kappa$, the initial condition imposes a congested state:

$$\mathbf{N}_{\text{c}_{\text{ini}}^{(i)}}(x, t) = \begin{cases} (i) & k_i(tw - x) - \kappa tw + b_i & : x_i + tw \leq x \leq x_{i+1} + tw \\ (ii) & k_c(tw - x) - \kappa tw + x_{i+1}(k_c - k_i) + b_i & : x_{i+1} + tw \leq x \leq x_{i+1} + tv_f \end{cases} \quad (33)$$

For an upstream boundary condition $\mathbf{N}_{\text{up}}^{(j)}$ as defined in (21), the solution component is expressed by:

$$\mathbf{N}_{\text{c}_{\text{up}}^{(j)}}(x, t) = \begin{cases} (i) & d_j + q_j(t - \frac{x-x_0}{v_f}) & : x_0 + v_f(t - t_{j+1}) \leq x \leq x_0 + v_f(t - t_j) \\ (ii) & d_j + q_j t_{j+1} + k_c((t - t_{j+1})v_f - (x - x_0)) & : x_0 \leq x \leq x_0 + v_f(t - t_{j+1}) \end{cases} \quad (34)$$

For a downstream boundary condition $\mathbf{N}_{\text{down}}^{(j)}$ as defined in (24), the solution component is expressed by:

$$\mathbf{N}_{\text{c}_{\text{down}}^{(j)}}(x, t) = \begin{cases} (i) & b_j + p_j t - (\frac{p_j}{w} + \kappa)(x_n - x) & : x_n + w(t - t_j) \leq x \leq x_n + w(t - t_{j+1}) \\ (ii) & b_j + p_j t_{j+1} + k_c((t - t_{j+1})v_f + x_n - x) & : x_n + w(t - t_{j+1}) \leq x \leq x_n \end{cases} \quad (35)$$

One can note that all solution components consist of two planar portions. The first one, numbered (i) in the solution component equations, is the characteristic domain as defined in 4.1.1, and is shaped as a trapezoid. The second one, noted (ii) in the same equations, is cone-shaped, and can represent either an expansion or a rarefaction wave. The characteristic domain propagates directly the density information from the value condition, at a characteristic speed v_f in free flow or w in congestion. On the cones, the density is the critical density and the flux is the maximum flux. An interesting point is that this does not depend on whether the cone is part of an expansion or a rarefaction wave. From a mathematical perspective, this comes from the linearity of R , and its constant derivative.

The algorithm we previously described would still be exact using these simplified formulas for the solution components. Nevertheless, the piecewise-linear shape of the solution components allows us to do several simplifications which yield noticeable improvements for the algorithmic complexity. Our approach to a fast algorithm has some similarities to what has been developed for the variational theory of traffic flow [13]: in particular, one can note that for a triangular fundamental diagram, the Lax-Hopf formula can be simplified to become the minimum of two elements, each of them representing a different information propagation speed. This remark yields considerable improvements for the computation of the Moskowitz function.

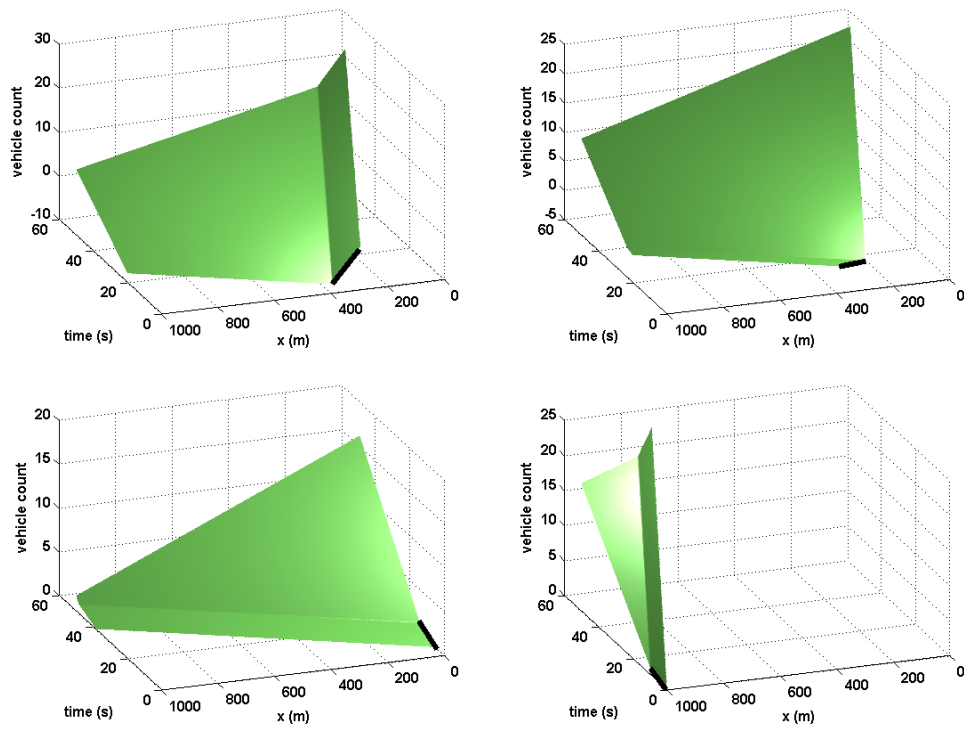


Figure 8: Three-dimensional representations of the solution components induced by local affine value conditions. **Top left:** solution component induced by a congested initial condition. **Top right:** solution component induced by a free-flow initial condition. **Bottom left:** solution component induced by an upstream boundary condition. **Bottom right:** solution component induced by a downstream boundary condition.

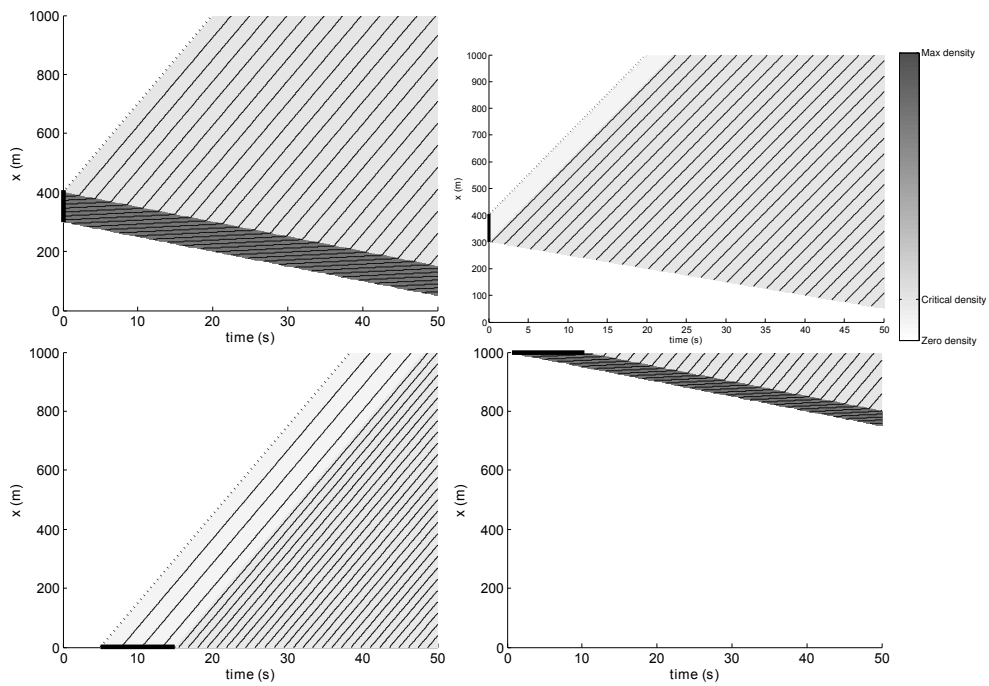


Figure 9: Two-dimensional representations of the solution components induced by local affine value conditions. Black curves represent isovalues of the Moskowitz function, and therefore vehicle trajectories. **Top left:** solution component induced by a congested initial condition. **Top right:** solution component induced by a free-flow initial condition. **Bottom left:** solution component induced by an upstream boundary condition. **Bottom right:** solution component induced by a downstream boundary condition.

5.2. Fast algorithm for well-posed problems

One can note two important properties of the solution components calculated previously

- The characteristic domains always propagate between speeds v_f and w
- The maximum capacity cones are all parts of parallel plans, since their gradient is $(v_f k_c, -k_c)$, and extend at any speed $u \in [w, v_f]$

These properties allow us to restrict the number of solution components we have to compute the Moskowitz function in one point (x, t) . Indeed, if the problem is well posed, the maximum capacity cones bring limited information since they all are parallel. Thus, we only have to compute the characteristic domains, which restricts the number of value conditions to inspect to two. This simplification yields Alg. 2.

Algorithm 2 Pseudo-code implementation for the Lax-Hopf based computation of the Moskowitz function and the associated density at a single point (x, t) for a triangular fundamental diagram.

Input: $t \in [0, t_n], x \in [x_0, x_m]$

$\mathbf{N} \leftarrow +\infty$

$i_{\text{up}} \leftarrow \max\{i | t_i \leq T - \frac{X-x_0}{v_f}\}$ {time index for influencing upstream boundary condition}

$i_{\text{down}} \leftarrow \max\{i | t_i \geq T - \frac{x_n-X}{w}\}$ {time index for influencing downstream boundary condition}

$j_{\text{min}} \leftarrow \min\{j - 1 | x_j \geq X - v_f T\}$ {space index for influencing initial condition}

$j_{\text{max}} \leftarrow \max\{j + 1 | x_j \leq X - w T\}$ {space index for influencing initial condition}

if $i_{\text{up}} \neq -\infty$ **then** {if at least one upstream condition influences (x, t) }

 compute $\mathbf{N}_{\mathbf{c}_{\text{up}}^{(i_{\text{up}})}(x, t)}$ using (34) {component induced by the upstream condition $\mathbf{c}_{\text{up}}^{(i_{\text{up}})}$ }

if $\mathbf{N} < \mathbf{N}_{\mathbf{c}_{\text{up}}^{(i_{\text{up}})}(x, t)}$ **then** {if the current component contributes to the solution}

$\mathbf{N} \leftarrow \mathbf{N}_{\mathbf{c}_{\text{up}}^{(i_{\text{up}})}(x, t)}$ {update Moskowitz function}

$k \leftarrow k_{\mathbf{c}_{\text{up}}^{(i_{\text{up}})}(x, t)}$, computed using (23) {compute density}

end if

end if

if $i_{\text{down}} \neq -\infty$ **then** {if at least one downstream condition influences (x, t) }

 compute $\mathbf{N}_{\mathbf{c}_{\text{down}}^{(i_{\text{down}})}(x, t)}$ using (35) {component induced by the downstream condition $\mathbf{c}_{\text{down}}^{(i_{\text{down}})}$ }

if $\mathbf{N} < \mathbf{N}_{\mathbf{c}_{\text{down}}^{(i_{\text{down}})}(x, t)}$ **then** {if the current component contributes to the solution}

$\mathbf{N} \leftarrow \mathbf{N}_{\mathbf{c}_{\text{down}}^{(i_{\text{down}})}(x, t)}$ {update Moskowitz function}

$k \leftarrow k_{\mathbf{c}_{\text{down}}^{(i_{\text{down}})}(x, t)}$, computed using (26) {compute density}

end if

end if

for $j_{\text{min}} \leq j \leq j_{\text{max}}$ **do** {iteration over initial conditions}

 compute $\mathbf{N}_{\mathbf{c}_{\text{ini}}^{(j)}(x, t)}$ using (32) or (33) {component induced by the initial condition $\mathbf{c}_{\text{ini}}^{(j)}$ }

if $\mathbf{N} < \mathbf{N}_{\mathbf{c}_{\text{ini}}^{(j)}(x, t)}$ **then** {if the current component contributes to the solution}

$\mathbf{N} \leftarrow \mathbf{N}_{\mathbf{c}_{\text{ini}}^{(j)}(x, t)}$ {update Moskowitz function}

$k \leftarrow k_{\mathbf{c}_{\text{ini}}^{(j)}(x, t)}$, computed using (20) {compute density}

end if

end for

Output: \mathbf{N}, k

6. Conclusion

This article develops an analytical expression of the entropy solution of the Lighthill-Whitham-Richards partial differential equation with an arbitrary flow-density relationship, and with piecewise constant initial

and boundary conditions. The analytical nature of the solution enables the construction of algorithms for exact solutions of the partial differential equation (up to machine accuracy) without numerical discretization error. The procedure is straightforward to implement, and has a low computational cost. It enables the computation of the solution at user prescribed points without gridding the space-time domain. We show that this method enable us to derive classical results for the density function and the cumulative number of vehicles function (its integral form). For the specific case of triangular flow-density relationships, we show that the proposed method can be reduced to a simpler and faster algorithm. Future work will deal with the use of the method for traffic flow estimation and/or control, for which some preliminary results have already been obtained [7] in the context of Lagrangian sensing.

ACKNOWLEDGMENTS

The authors are grateful to Professor Lawrence Craig Evans for his guidance on the treatment of nonsmoothness arising in solutions to Hamilton-Jacobi equations, and to Professor Jean-Pierre Aubin for his guidance and vision, and for his help to pose the Hamilton-Jacobi problem as a viability problem. Professor Carlos Daganzo is gratefully acknowledged for his guidance on traffic flow engineering. The authors want to express their warmest thanks to Professor Patrick Saint-Pierre for his initial guidance in generating code for numerical solutions of the HJ PDE. The numerical computations presented in this work have been done using technologies initially developed by the company VIMADES.

References

- [1] E. ANGEL and R.E. BELLMAN. *Dynamic programming and partial differential equations*. Academic Press, New York, NY, 1972.
- [2] R. ANSORGE. What does the entropy condition mean in traffic flow theory? *Transportation Research*, 24B(2):133–143, 1990.
- [3] J.-P. AUBIN. *Viability Theory*. Systems and Control: Foundations and Applications. Birkhäuser, Boston, MA, 1991.
- [4] J.-P. AUBIN, A. M. BAYEN, and P. SAINT-PIERRE. Dirichlet problems for some Hamilton-Jacobi equations with inequality constraints. *SIAM Journal on Control and Optimization*, 47(5):2348–2380, 2008.
- [5] C. BARDOS, A. Y. LEROUX, and J. C. NEDELEC. First order quasilinear equations with boundary conditions. *Communications in partial differential equations*, 4(9):1017–1034, 1979.
- [6] S. BLANDIN, D. WORK, P. GOATIN, B. PICCOLI, and A. BAYEN. A general phase transition model for vehicular traffic. *Conditionally accepted to the SIAM journal on Applied Mathematics*, 2009.
- [7] C. G. CLAUDEL and A. M. BAYEN. Convex formulations of data assimilation problems for a class of Hamilton-Jacobi equations. *Submitted to the SIAM Journal on Control and Optimization*, 2009.
- [8] C. G. CLAUDEL and A. M. BAYEN. Lax-Hopf based incorporation of internal boundary conditions into Hamilton-Jacobi equation. Part I: theory. *IEEE Transactions on Automatic Control*, 55(5):1142–1157, 2010. doi:10.1109/TAC.2010.2041976.
- [9] C. G. CLAUDEL and A. M. BAYEN. Lax-Hopf based incorporation of internal boundary conditions into Hamilton-Jacobi equation. Part II: Computational methods. *IEEE Transactions on Automatic Control*, 55(5):1158–1174, 2010. doi:10.1109/TAC.2010.2045439.
- [10] C. F. DAGANZO. The cell transmission model: a dynamic representation of highway traffic consistent with the hydrodynamic theory. *Transportation Research*, 28B(4):269–287, 1994.
- [11] C. F. DAGANZO. The cell transmission model, part II: network traffic. *Transportation Research*, 29B(2):79–93, 1995.
- [12] C. F. DAGANZO. A variational formulation of kinematic waves: Solution methods. *Transportation Research Part B*, 39(10):934–950, 2005.
- [13] C. F. DAGANZO. A variational formulation of kinematic waves: basic theory and complex boundary conditions. *Transportation Research B*, 39B(2):187–196, 2005.
- [14] C. F. DAGANZO. On the variational theory of traffic flow: well-posedness, duality and applications. *Networks and heterogeneous media*, 1(4):601–619, 2006.
- [15] L.C. EDIE. Car-following and steady-state theory for noncongested traffic. *Operations Research*, 9(1):66–76, 1961.
- [16] L. C. EVANS. *Partial Differential Equations*. American Mathematical Society, Providence, RI, 1998.
- [17] M. GARAVELLO and B. PICCOLI. *Traffic flow on networks*. American Institute of Mathematical Sciences, Springfield, MO, 2006.
- [18] N. GEROLIMINIS and C. F. DAGANZO. Existence of urban-scale macroscopic fundamental diagrams: Some experimental findings. *Transportation Research Part B: Methodological*, 42(9):759–770, 2008.
- [19] S. K. GODUNOV. A difference method for numerical calculation of discontinuous solutions of the equations of hydrodynamics. *Math. Sbornik*, 47:271–306, 1959.
- [20] B. D. GREENSHIELDS. A study of traffic capacity. *Proc. Highway Res. Board*, 14:448–477, 1935.

- [21] V. HENN. A wave-based resolution scheme for the hydrodynamic LWR traffic flow model. In Bovy Schreckenberg Wolf Hoogendoorn, Luding, editor, *Proceedings of the Workshop on Traffic and Granular Flow 03*, pages 105–124, Amsterdam, 2003.
- [22] B. Hoh, M. Gruteser, R. Herring, J. Bana, D. Work, J-C. Herrera, A. M. Bayen, M. Annavaramb, and Q. Jacobsonc. Virtual trip lines for distributed privacy-preserving traffic monitoring. *International Conference on Mobile Systems, Applications and Services*, 2008.
- [23] B. HULL, V. BYCHKOVSKY, Y. ZHANG, K. CHEN, M. GORACZKO, A. MIU, E. SHIH, H. BALAKRISHNAN, and S. MADDEN. CarTel: a distributed mobile sensor computing system. In *Proceedings of the 4th international conference on Embedded networked sensor systems*, pages 125–139. ACM, 2006.
- [24] B. S. KERNER and P. KONHÄUSER. Structure and parameters of clusters in traffic flow. *Phys. Rev. E*, 50(1):54–83, Jul 1994.
- [25] L. LECLERCQ, S. CHANUT, and J. B. LESORT. Moving Bottlenecks in Lighthill-Whitham-Richards Model: A Unified Theory. *Transportation Research Record*, 1883:3–13, 2004.
- [26] P. LE FLOCH. Explicit formula for scalar non-linear conservation laws with boudary condition. *Math. Meth. Appl. Sci.*, 10:265–287, 1988.
- [27] M. J. LIGHTHILL and G. B. WHITHAM. On kinematic waves. II. A theory of traffic flow on long crowded roads. *Proceedings of the Royal Society of London*, 229(1178):317–345, 1956.
- [28] Y. LU, SC WONG, M. ZHANG, C.W. SHU, and W. CHEN. Explicit construction of entropy solutions for the Lighthill-Whitham-Richards traffic flow model with a piecewise quadratic flow-density relationship. *Transportation Research Part B: Methodological*, 42(4):355–372, 2008.
- [29] Y. MAKIGAMI, G. F. NEWELL, and R. ROTHERY. Three-dimensional representation of traffic flow. *Transportation Science*, 5(3):303–313, Aug 1971.
- [30] K. MOSKOWITZ. Discussion of ‘freeway level of service as influenced by volume and capacity characteristics’ by D.R. Drew and C. J. Keese. *Highway Research Record*, 99:43–44, 1965.
- [31] L. MUNOZ, X. SUN, G. GOMES, and R. HOROWITZ. Methodological calibration of the cell transmission model. In *American Control Conference*, Boston, MA, June 2004.
- [32] G. F. NEWELL. A simplified theory of kinematic waves in highway traffic, Part (I), (II) and (III). *Transportation Research B*, 27B(4):281–313, 1993.
- [33] P. I. RICHARDS. Shock waves on the highway. *Operations Research*, 4(1):42–51, 1956.
- [34] I. S. STRUB and A. M. BAYEN. Weak formulation of boundary conditions for scalar conservation laws. *International Journal of Robust and Nonlinear Control*, 16:733–748, 2006.
- [35] P. VARAIYA. Reducing highway congestion: an empirical approach. *European Journal of Control*, 11(4-5):1–9, 2005.
- [36] Y. WANG and M. PAPAGEORGIOU. Real-time freeway traffic state estimation based on extended Kalman filter: a general approach. *Transportation Research Part B*, 39(2):141–167, 2005.
- [37] <http://traffic.berkeley.edu/downloads/>.

A. Appendix: Lipschitz-continuity of the solution

Lemma A.1. *Let $f, g : A \mapsto B$ be two Lipschitz-continuous functions. Then $h : x \rightarrow \min\{f(x), g(x)\}$ is Lipschitz-continuous on A .*

Proof — We remark that $2 \cdot \min(a, b) = a + b - |a - b|$, therefore h is a linear combination of Lipschitz-continuous functions. Hence, it is Lipschitz-continuous. \square

For notational convenience in the Appendix, we use $\mathbf{c}^{(i)}$ as a generic notation for $\mathbf{c}_{\text{ini}}^{(i)}$, $\mathbf{c}_{\text{up}}^{(j)}$, $\mathbf{c}_{\text{down}}^{(j)}$ through this appendix.

Definition A.2. *Let $\mathbf{N}_{\mathbf{c}^{(i)}}$ be a solution component. We define the upper-boundary extension $\widehat{\mathbf{N}}^{(i)}$ of $\mathbf{N}_{\mathbf{c}^{(i)}}$ the following way: If $\mathbf{N}_{\mathbf{c}^{(i)}}$ is a component induced by an initial boundary condition as defined in (10), i.e. $\mathbf{c}^{(i)} = \mathbf{c}_{\text{ini}}^{(i)}$, then*

$$\widehat{\mathbf{N}}_{\mathbf{c}^{(i)}}(x, t) = \begin{cases} \mathbf{N}_{\mathbf{c}^{(i)}}(x, t) & : \text{if } (x, t) \in \text{Dom}(\mathbf{N}^{(i)}) \\ \mathbf{N}_{\mathbf{c}^{(i)}}(x_{i+1} + tv_f, t) & : \text{if } x > x_{i+1} + tv_f \\ \mathbf{N}_{\mathbf{c}^{(i)}}(x_i + tw, t) + (x_i + tw - x)\kappa & : \text{if } x < x_i + tw \end{cases} \quad (36)$$

If $\mathbf{N}_{\mathbf{c}^{(i)}}$ is induced by an upstream boundary condition as defined in (11) i.e. $\mathbf{c}^{(i)} = \mathbf{c}_{\text{up}}^{(i)}$, then

$$\widehat{\mathbf{N}}_{\mathbf{c}^{(i)}}(x, t) = \begin{cases} \mathbf{N}_{\mathbf{c}^{(i)}}(x, t) & : \text{if } (x, t) \in \text{Dom}(\mathbf{N}_{\mathbf{c}^{(i)}}) \\ \mathbf{N}_{\mathbf{c}^{(i)}}(x, t_i + \frac{x-x_0}{v_f}) & : \text{if } (x, t) \notin \text{Dom}(\mathbf{N}_{\mathbf{c}^{(i)}}) \end{cases} \quad (37)$$

If $\mathbf{N}_{\mathbf{c}^{(i)}}$ is induced by a downstream boundary condition as defined in (12) i.e. $\mathbf{c}^{(i)} = \mathbf{c}_{\text{down}}^{(i)}$, then

$$\widehat{\mathbf{N}}_{\mathbf{c}^{(i)}}(x, t) = \begin{cases} \mathbf{N}_{\mathbf{c}^{(i)}}(x, t) & : \text{if } (x, t) \in \text{Dom}(\mathbf{N}_{\mathbf{c}^{(i)}}) \\ \mathbf{N}_{\mathbf{c}^{(i)}}(x, t_i + \frac{x-x_n}{w}) + (t_i + \frac{x-x_n}{w} - t)q_{\text{max}} & : \text{if } (x, t) \notin \text{Dom}(\mathbf{N}_{\mathbf{c}^{(i)}}) \end{cases} \quad (38)$$

The interpretation of the upper-boundary extensions is as follows. Downstream from the free flow characteristic line, the solution component is extended with isolines parallel to the x axis, which corresponds to no cars added downstream. Upstream from the characteristic line with slope w emanating from $(x_k, 0)$, the solution component induced by an initial condition $\mathbf{c}_{\text{ini}}^{(k)}$ is extended so that the corresponding density is the jam density κ at any time. Similarly, the solution component induced by a downstream condition is extended so that the corresponding flow is the maximum flow q_{max} . Note that these two parts of the upper-boundary extensions do not satisfy the Hamilton-Jacobi PDE. This mathematical argument does not pose any problem since another component will fill the corresponding area, with a smaller value (the extension on this side of the domain is only required for the mathematical proof of Lipschitz-continuity). Thus, by the Lax-Hopf formula, the extensions do not change the nature of the solution. One can note that every function $\widehat{\mathbf{N}}_{\mathbf{c}^{(i)}}$ is designed to be defined and Lipschitz-continuous on the entire domain $[x_0, x_n] \times [0, t_m]$, and to coincide with $\mathbf{N}_{\mathbf{c}^{(i)}}$ when the latter is defined.

Lemma A.3.

$$\forall x \in [x_0, x_n], \forall t \in [0, t_m], \quad \min_{0 \leq i < n} \widehat{\mathbf{N}}_{\mathbf{c}_{\text{ini}}^{(i)}}(x, t) = \min_{i \text{ s.t. } 0 \leq i < n \text{ and } (x, t) \in \text{Dom}(\mathbf{N}_{\mathbf{c}_{\text{ini}}^{(i)}})} \mathbf{N}_{\mathbf{c}_{\text{ini}}^{(i)}}(x, t) \quad (39)$$

Proof — Let $x \in [x_0, x_n], t \in [0, t_m]$ be fixed for the entire proof. We define $r_{\text{min}} = \max\{k | x_k \leq x - v_f t\}$ and $r_{\text{max}} = \max\{k | x_k \leq x - wt\}$, then $\forall r \in \{r_{\text{min}}, \dots, r_{\text{max}}\}, (x, t) \in \text{Dom}(\mathbf{N}_{\mathbf{c}_{\text{ini}}^{(r)}})$: thus every point (x, t) lies in the domain of at least one solution component induced by an initial condition.

The Lax-Hopf formula (14) gives

$$\mathbf{N}_{\mathbf{c}_{\text{ini}}^{(k)}}(x_k + tw, t) \geq \mathbf{N}_{\mathbf{c}_{\text{ini}}^{(k-1)}}(x_k + tw, t) \quad (40)$$

as long as $x_k + tw \in [x_0, x_n]$ and $t \in [0, t_m]$. This is due to the fact that the point $(x_k + tw, t)$ can be reached by more than one characteristic induced by $\mathbf{c}_{\text{ini}}^{(k-1)}$.

Let $k > r_{\text{max}}$, then we have $x < x_k + tw$ and $(x, t) \notin \text{Dom}(\mathbf{N}_{\mathbf{c}_{\text{ini}}^{(k)}})$. In respective order, the definition of the upper-boundary extension, the property (40), the fact that $\mathbf{N}_{\mathbf{c}_{\text{ini}}^{(k-1)}}(x_k + tw, t) = \widehat{\mathbf{N}}_{\mathbf{c}_{\text{ini}}^{(k-1)}}(x_k + tw, t)$, and that $\widehat{\mathbf{N}}_{\mathbf{c}_{\text{ini}}^{(k-1)}}(\cdot, t)$ is κ -Lipschitz, yield

$$\begin{aligned} \widehat{\mathbf{N}}_{\mathbf{c}_{\text{ini}}^{(k)}}(x, t) &= \mathbf{N}_{\mathbf{c}_{\text{ini}}^{(k)}}(x_k + tw, t) + (x_k + tw - x)\kappa \\ &\geq \mathbf{N}_{\mathbf{c}_{\text{ini}}^{(k-1)}}(x_k + tw, t) + (x_k + tw - x)\kappa \\ &\geq \widehat{\mathbf{N}}_{\mathbf{c}_{\text{ini}}^{(k-1)}}(x_k + tw, t) + (x_k + tw - x)\kappa \\ &\geq \widehat{\mathbf{N}}_{\mathbf{c}_{\text{ini}}^{(k-1)}}(x, t) \end{aligned}$$

Therefore $\forall k > r_{\text{max}}, \widehat{\mathbf{N}}_{\mathbf{c}_{\text{ini}}^{(k)}}(x, t) \geq \widehat{\mathbf{N}}_{\mathbf{c}_{\text{ini}}^{(k-1)}}(x, t)$. By induction on k , and using the fact that $\widehat{\mathbf{N}}_{\mathbf{c}_{\text{ini}}^{(r_{\text{max}})}}(x, t) = \mathbf{N}_{\mathbf{c}_{\text{ini}}^{(r_{\text{max}})}}(x, t)$ because $(x, t) \in \text{Dom}(\mathbf{N}_{\mathbf{c}_{\text{ini}}^{(r_{\text{max}})}})$,

$$\min_{r_{\text{max}} \leq i < n} \widehat{\mathbf{N}}_{\mathbf{c}_{\text{ini}}^{(i)}}(x, t) = \mathbf{N}_{\mathbf{c}_{\text{ini}}^{(r_{\text{max}})}}(x, t) \quad (41)$$

The Lax-Hopf formula (14) also gives

$$\mathbf{N}_{\mathbf{c}_{\text{ini}}^{(k-1)}}(x_k + tv_f, t) \geq \mathbf{N}_{\mathbf{c}_{\text{ini}}^{(k)}}(x_k + tv_f, t) \quad (42)$$

Let $k \leq r_{\min}$ such that $(x, t) \notin \text{Dom}(\mathbf{N}_{\mathbf{c}_{\text{ini}}^{(k-1)}})$, then $x > x_k + tv_f$. Similarly as for the first case, the definition of the upper-boundary extension, the property (42), the fact that $\widehat{\mathbf{N}}_{\mathbf{c}_{\text{ini}}^{(k)}}(\cdot, t)$ is a decreasing function, respectively give the following set of inequalities.

$$\begin{aligned} \widehat{\mathbf{N}}_{\mathbf{c}_{\text{ini}}^{(k-1)}}(x, t) &= \mathbf{N}_{\mathbf{c}_{\text{ini}}^{(k-1)}}(x_k + tv_f, t) \\ &\geq \mathbf{N}_{\mathbf{c}_{\text{ini}}^{(k)}}(x_k + tv_f, t) \\ &\geq \widehat{\mathbf{N}}_{\mathbf{c}_{\text{ini}}^{(k)}}(x_k + tv_f, t) \\ &\geq \widehat{\mathbf{N}}_{\mathbf{c}_{\text{ini}}^{(k)}}(x, t) \end{aligned}$$

Therefore $\forall k \leq r_{\min}$, $\widehat{\mathbf{N}}_{\mathbf{c}_{\text{ini}}^{(k-1)}}(x, t) \geq \widehat{\mathbf{N}}_{\mathbf{c}_{\text{ini}}^{(k)}}(x, t)$. By induction on k , and using the fact that $\widehat{\mathbf{N}}_{\mathbf{c}_{\text{ini}}^{(r_{\min})}}(x, t) = \mathbf{N}_{\mathbf{c}_{\text{ini}}^{(r_{\min})}}(x, t)$ because $(x, t) \in \text{Dom}(\mathbf{N}_{\mathbf{c}_{\text{ini}}^{(r_{\min})}})$,

$$\min_{0 \leq i \leq r_{\min}} \widehat{\mathbf{N}}_{\mathbf{c}_{\text{ini}}^{(i)}}(x, t) = \mathbf{N}_{\mathbf{c}_{\text{ini}}^{(r_{\min})}}(x, t) \quad (43)$$

Since $\forall k \in \{r_{\min}, \dots, r_{\max}\}$, $(x, t) \in \text{Dom}(\mathbf{N}_{\mathbf{c}_{\text{ini}}^{(k)}})$, equations (41) and (43) give:

$$\exists r \in \{r_{\min}, \dots, r_{\max}\} : \mathbf{N}_{\mathbf{c}_{\text{ini}}^{(r)}}(x, t) = \min_{0 \leq i \leq n} \widehat{\mathbf{N}}_{\mathbf{c}_{\text{ini}}^{(i)}}(x, t)$$

This last equality concludes the proof of equation (39) of the lemma. \square

This proves that for initial conditions the upper boundary extension of the components does not modify the final solution.

Proposition A.4.

$$\forall x \in [x_0, x_n], \forall t \in [0, t_m], \quad \min_i \widehat{\mathbf{N}}_{\mathbf{c}_{\text{ini}}^{(i)}}(x, t) = \min_{i \text{ s.t. } (x, t) \in \text{Dom} \mathbf{N}_{\mathbf{c}_{\text{ini}}^{(i)}}} \mathbf{N}_{\mathbf{c}_{\text{ini}}^{(i)}}(x, t)$$

Proof — Lemma A.3 states that the above equality holds when one only considers initial boundary conditions. We use the same method to prove the continuity of the entire solution. Let $x \in [x_0, x_n], \forall t \in [0, t_m]$ be fixed for the entire proof. Let $j > 0$ such that $(x, t) \notin \text{Dom} \mathbf{N}_{\mathbf{c}_{\text{up}}^{(j)}}$. The same process as previously, knowing that $\widehat{\mathbf{N}}_{\mathbf{c}_{\text{up}}^{(j-1)}}(x, \cdot)$ is q_{\max} -Lipschitz, gives

$$\begin{aligned} \widehat{\mathbf{N}}_{\mathbf{c}_{\text{up}}^{(j)}}(x, t) &= \mathbf{N}_{\mathbf{c}_{\text{up}}^{(j)}}\left(x, t_j + \frac{x - x_0}{v_f}\right) + \left(t_j + \frac{x - x_0}{v_f} - t\right) q_{\max} \\ &\geq \mathbf{N}_{\mathbf{c}_{\text{up}}^{(j-1)}}\left(x, t_j + \frac{x - x_0}{v_f}\right) + \left(t_j + \frac{x - x_0}{v_f} - t\right) q_{\max} \\ &\geq \widehat{\mathbf{N}}_{\mathbf{c}_{\text{up}}^{(j-1)}}(x, t) \end{aligned}$$

If $(x, t) \notin \text{Dom}\mathbf{N}_{\mathbf{c}_{\text{up}}^{(0)}}$, one can prove similarly that:

$$\begin{aligned}\widehat{\mathbf{N}}_{\mathbf{c}_{\text{up}}^{(0)}}(x, t) &= \mathbf{N}_{\mathbf{c}_{\text{up}}^{(0)}}\left(x, \frac{x-x_0}{v_f}\right) + \left(\frac{x-x_0}{v_f} - t\right) q_{\text{max}} \\ &\geq \mathbf{N}_{\mathbf{c}_{\text{ini}}^{(0)}}\left(x, \frac{x-x_0}{v_f}\right) + \left(\frac{x-x_0}{v_f} - t\right) q_{\text{max}} \\ &\geq \widehat{\mathbf{N}}_{\mathbf{c}_{\text{ini}}^{(0)}}(x, t)\end{aligned}$$

Because any point (x, t) is on a characteristic curve emanating from $(x, 0)$, there exists i such that $(x, t) \in \text{Dom}(\mathbf{N}_{\mathbf{c}^{(i)}})$. Furthermore, because of the two previous inequalities, we can extend this statement to the following statement: there exists i such that $(x, t) \in \text{Dom}\mathbf{N}_{\mathbf{c}^{(i)}}$ and $\widehat{\mathbf{N}}_{\mathbf{c}_{\text{up}}^{(j)}}(x, t) \geq \mathbf{N}^{(i)}(t, x)$. The same induction as before gives

$$\exists r : \mathbf{N}_{\mathbf{c}^{(r)}}(x, t) = \min\left(\left\{\widehat{\mathbf{N}}_{\mathbf{c}_{\text{ini}}^{(i)}}(x, t) \mid 0 \leq i < n\right\} \cup \left\{\widehat{\mathbf{N}}_{\mathbf{c}_{\text{up}}^{(j)}}(x, t) \mid 0 \leq j < m\right\}\right)$$

Symmetrically for downstream conditions, we can generate the same results: we know that if $(x, t) \notin \text{Dom}\mathbf{N}_{\mathbf{c}_{\text{down}}^{(j)}}$, $\widehat{\mathbf{N}}_{\mathbf{c}_{\text{down}}^{(j)}}(x, t) \geq \widehat{\mathbf{N}}_{\mathbf{c}_{\text{down}}^{(j-1)}}(x, t)$ and if $(x, t) \notin \text{Dom}\mathbf{N}_{\mathbf{c}_{\text{down}}^{(0)}}$, $\widehat{\mathbf{N}}_{\mathbf{c}_{\text{down}}^{(0)}}(x, t) \geq \widehat{\mathbf{N}}_{\mathbf{c}_{\text{ini}}^{(n-1)}}(x, t)$. Therefore, $\exists i : (x, t) \in \text{Dom}\mathbf{N}_{\mathbf{c}^{(i)}}$ and $\widehat{\mathbf{N}}_{\mathbf{c}_{\text{down}}^{(j)}}(x, t) \geq \mathbf{N}_{\mathbf{c}^{(i)}}(t, x)$. A quick induction then shows that

$$\min_{i \text{ s.t. } (x, t) \in \text{Dom}\mathbf{N}_{\mathbf{c}^{(i)}}} \widehat{\mathbf{N}}_{\mathbf{c}^{(i)}}(x, t) = \min_i \mathbf{N}_{\mathbf{c}^{(i)}}(x, t)$$

□

Theorem A.5. *Let us consider the Cauchy problem as stated in equation (6). If the imposed initial densities are in $[0, \kappa]$ and if the imposed upstream and downstream flows are in $[0, q_{\text{max}}]$, then the solution to the Cauchy problem is Lipschitz-continuous.*

Proof — We apply lemma (A.1) to the result of proposition (A.4). □